

Bio-oil production from fast pyrolysis of furniture processing residue

Hoang Vu Ly^{*,**}, Quoc Khanh Tran^{*}, Byung Hee Chun^{*}, Changho Oh^{***}, Jinsoo Kim^{**,†}, and Seung-Soo Kim^{*,†}

^{*}Department of Chemical Engineering, Kangwon National University, 346 Joongang-ro, Samcheok, Gangwon-do 25913, Korea

^{**}Department of Chemical Engineering (Integrated Engineering), Kyung Hee University, 1732 Deogyong-daero, Giheung-gu, Yongin, Gyeonggi-do 17104, Korea

^{***}Daekyung Esco, M-1903, 32, Songdowahak-ro, Yeonsu-gu, Incheon 21984, Korea

(Received 16 June 2020 • Revised 25 September 2020 • Accepted 3 October 2020)

Abstract—The pyrolysis characteristic of furniture processing residue (FPR), which was analyzed by thermogravimetric analysis (TGA) under nitrogen atmosphere, mainly decomposed between 230 °C and 500 °C. The FPR was submitted to fast pyrolysis in a bubbling fluidized-bed reactor (BFR) for converting into bio-oil, bio-char. The product distribution and characteristics of bio-oil depend on the operating conditions (temperature, fluidizing flow rate, particle size of sample). The bio-oil yield showed the highest value (50.68 wt%) at the pyrolysis temperature of 450 °C with a biomass particle size of 1.0 mm and a fluidization velocity of $2.0 \times U_{mf}$. The bio-oil had high selectivity for dioctyl phthalate, levoglucosan, and phenolic derivatives. The carbon number proportions in bio-oils of FPR were 32.74 wt% for C₅-C₁₁ fraction, 47.60 wt% for C₁₂-C₁₈ fraction and 19.38 wt% of C₂₅-C₃₈ fraction, respectively. The gas product included CO, CO₂, H₂, and hydrocarbons (C₁-C₄), and the selectivity of CO₂ was the highest. The high heating value (HHV) of gas products was between 4.60 and 12.90 MJ/m³. The bio-char shows high HHV (23.87 MJ/kg) and high C content (62.47 wt%) that can be applied as a solid fuel.

Keywords: Furniture Processing Residue, Fast Pyrolysis, Fluidized-bed Reactor, Bio-char, Bio-oil

INTRODUCTION

Utilization of the limited fossil sources for our daily life has resulted in global warming with the discharges of greenhouse gases, impacting on the climate and human life [1-3]. Consequently, the research for renewable resources to replace fossil resources has received great attention. Biomass has been considered as an attractive renewable source, as it can be used to produce heat, power, or chemicals, transportation fuels and biomaterials [1-4]. Biomass is converted into energy via the thermal conversion processes, including three main techniques: combustion, pyrolysis, and gasification. These are prevailing methods that convert biomass efficiently and economically into energy [1]. Pyrolysis is the most promising approach and widely used for production of biofuels and chemicals from biomass materials [4]. The pyrolysis process can be classified into slow, fast and flash pyrolysis [4]. Fast pyrolysis, which is preferred for bio-oil production, is a decomposition process of organic materials in atmospheric conditions and lack of oxygen at moderate temperature (around 500 °C) with high heating rate and short residence time [3,5]. Technically, the pyrolysis process produces bio-oil which can be used as raw material to produce gasoline, diesel or chemicals [6]. The solid residue after pyrolysis is known as bio-char that can be utilized as materials for electrochemistry to produce bio-char battery or fertilizer to amend soil solid fuel [6].

The research on pyrolysis has progressed with diverse biomass samples derived from different generation biofuel feedstock, namely

agricultural residue [6,7], wood plant [3,8,9], macroalgae [4,10,11]. Woody biomass is an interesting alternative due to advantages over other biomass, e.g., high energy, but low costs, low ash content, and very low nitrogen and sulfur content [3]. Forest residue, especially secondary woody residue, generated as by-products from wood processing industries, includes sawdust, shavings, woodchips, and tree bark [12]. It is considered as a potential material for energy recovery. The utilization of wood processing residue for biofuel production has been of more interest because of environmental and economic impact. Azargohar et al. [6] investigated the effect of pyrolysis temperature on the properties of products using four types of waste: wheat straw, saw dust, flax straw and poultry litter. Saw dust had the highest bio-oil yield 52 wt% compared to those of the others. Papari et al. [13] investigated the pyrolysis of sawmill residue (hardwood sawdust, softwood shavings and softwood bark) in an auger reactor for optimizing the reaction temperature to collect the highest yield of bio-oil and properties of bio-oil. For bio-char production, Solar et al. [14] studied the pyrolysis of woody biomass wastes (forest residue) in auger screw reactor. The char product is used as a reductant in metallurgical applications. Morali et al. [3] examined the pyrolysis of sawdust residue from a hardwood tree (*Hornbeam*, *Carpinus betulus* L.) in fixed-bed reactor at 400-600 °C, for both bio-oil and bio-char production. For the performance of pyrolysis in a larger-scale system, the fluidized-bed reactor (FR) system is preferred due to the continuous feeding of solid material without shutting down the system and the good heat-transfer between the biomass, bed material, and reactor walls.

In this work, the fast pyrolysis of FPR from furniture industry was carried out in BFR under different conditions to investigate the influence of these operating factors on product distribution and

[†]To whom correspondence should be addressed.

E-mail: jkim21@khu.ac.kr, sskim2008@kangwon.ac.kr

Copyright by The Korean Institute of Chemical Engineers.

Table 1. Characteristics of FPR samples

Proximate analysis (wt%)	Moisture ^a	Ash ^b	Volatile matter ^c	Fixed carbon ^c	Elemental analysis ^d (wt%)					HHV (MJ/kg) d.a.f.b
					C	H	N	S	O ^e	
Furniture processing residue	5.62±0.05	10.54±0.45	68.50	15.34	48.54	5.90	2.65	0.13	42.78	17.68

^aASTM E1756, Standard test method for the determination of the total solids of biomass.

^bASTM E1755, Standard test method for determination of ash content of biomass.

^cCalculating based on sample after drying.

^dOn dry, ash free basis.

^eBy difference.

properties of bio-oils. The physiochemical characteristics of bio-oil and bio-char were analyzed using various techniques.

EXPERIMENTAL PROCEDURE

1. Materials and Initial Characterization

The FPR was provided by Hanssem Co. LTD. (Korea). The biomass sample was crushed by knife mill (RT-08, MHK Co.) and sieved to divide into three fractions: (0.4-0.6), (0.8-1.2), and (1.3-1.7) mm in length. The proximate analyses of sample were determined following ASTM standard method [9]. The moisture of sample should be lower than 10 wt%, to ensure rapid heating as well as minimize the moisture content in the liquid product [15]. Therefore, before being used for experiment, the FPR samples were dried for 12 h in the oven at 105 °C.

Thermogravimetric (TG) analysis was performed to evaluate the thermal degradation of biomass and understand the pyrolysis characteristics of materials. For this, 3-5 mg of sample was heated from room temperature to 700 °C at 10 °C/min in N₂ environment (20 mL/min) in a TG analyzer (N-1000, SINCO).

2. Setup and Analytical Methods

The experiments were performed in BFR under nitrogen atmosphere with silica sand (particle size of 150-212 μm) as the bed material. The reaction temperature was chosen from TGA data. The gas velocity ranged from 1.5 to 4.0×U_{mf} (with U_{mf}=5.0 L/min), which is equivalent to a pressure range of 0.51-0.57 kPa in a fluidized-bed. The schematic of the reactor system was specifically reported in our previous literature [4,9]. The product distributions were calculated based on the weight of each product produced after reaction and amount of fed biomass sample.

The element analysis to characterize the C, H, N, O concentration of bio-char and bio-oil was determined by CE Instrument analyzer (Flash EA1112) [4,10]. The pH of liquid products was measured with pH meter (Thermo Scientific Orion 3-Star), while the moisture content was analyzed using Karl-Fischer (TL, 7500KF), respectively. The bio-oil (organic phase) and aqueous phase were separated from liquid product. The organic compounds in the bio-oil were identified by gas chromatograph coupled with mass spectrometry (GC-MS, Agilent 7890A/5975C) with a HP-5MS capillary column (30 m×0.25 mm×0.25 μm), with a helium gas stream of 1.0 ml/min. The initial temperature of the oven was set at 40 °C. Then, the temperature was raised to 250 °C at a 10 °C/min and kept for 10 min. The injector volume was 1 μl and temperature of injector was kept constant at 280 °C. The bio-oil was dissolved in dimethyl

sulfoxide-d6 solvent (DMSO-d6) before being analyzed by NMR spectroscopy (300 MHz NMR spectrometer) to identify the different functional groups present in the organic compounds.

The gas products that flowed from system were directly analyzed and quantified by gas chromatography (YL 6500GC). The gas components were separated using Porapak N and Molecular sieve 13X column. The signals of gas compositions were detected by a flame ionization detector (FID), with nitrogen sweeper gas (20 mL/min) and a mixture of pure hydrogen (30 mL/min) and pure air (300 mL/min) to keep the flame lighted, and a thermal conductivity detector (TCD) using 20 mL/min of argon carrier gas (99.999% purity).

RESULTS AND DISCUSSION

1. Characterization of Material

The physical and chemical characteristics of FPR are reported in Table 1. The moisture of FPR was 5.62 wt%. This value is reasonable for the pyrolysis process. The ash content was 10.54 wt%, which was higher than pine tree [8], tulip tree [9], or woody biomass without bark [6]. The chemical element analysis of FPR biomass exhibited the C, H, N, and O content of 43.42, 5.78, 2.60, and 48.20 wt% on a dry, ash free basis (d.a.f.b). The HHV of FPR was calculated based on the concentrations (wt%) of C, H, N, and O according to Demirbas's equation [9,16]. The HHV of FPR was 17.68 MJ/kg, which is similar to *Pinyon* pine (18.94 MJ/kg) [8], or *Pinus pinaster* (15.70 MJ/kg) [14].

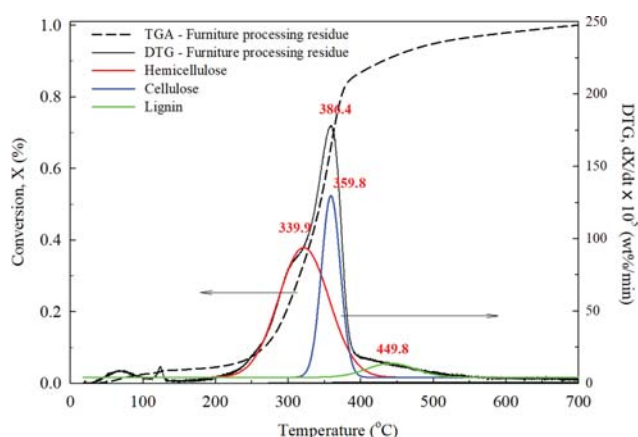


Fig. 1. Thermogravimetric (TG) and differential thermogravimetric (DTG) curves for the FPR and main components of FPR at heating rate of 10 °C/min.

2. Thermogravimetric Analysis of FPR

The TGA signal was obtained from the mass change of FPR with temperature in thermolysis. It can be represented as a function of the conversion X , which is calculated following the conversion equation in previous literature [9,17].

The TGA and DTG behavior of FPR was comparable to that of lignocellulosic biomass, as shown in Fig. 1. A small signal appearing between 0 and 150 °C was due to the evaporation of moisture and degradation of extractives in sample. The small shoulder peak in the range 200–250 °C can be considered as the thermal desorption zone of phthalates (which was used as additive in wood products) [18]. The major thermal conversion of FPR occurred in a temperature range between 230 and 500 °C, with the maximum decomposition at 358.4 °C. The DTG profile in this zone was separated into three main distinct peaks. The first peak, at 319.9 °C, was probably due to the hemicellulose decomposition. The second peak, at 359.8 °C, corresponded to the degradation of cellulose. The lignin component decomposed in a wide temperature range and showed the peak at 439.8 °C [8,19].

3. Pyrolysis Product Distribution

3-1. Effect of Temperature

Reaction temperature is considered as the most significant factor in bio-oil production process due to its influence on the decomposition of biomass bonds in pyrolysis. As the reaction temperature rises to much higher temperature, the volatile vapor may be cracked into gas through the secondary reactions, resulting in higher gas yield [9,10]. The FPR was pyrolyzed in BFR at temperature between 400 °C and 550 °C. Table 2 presents the product distributions ob-

tained at different pyrolysis temperatures. Initially, the liquid yield increased from 46.02 wt% (at 400 °C) to 50.68 wt% (at 450 °C) and then decreased to 43.08 wt% (at 550 °C). Meanwhile, the char yield decreased from 37.62 to 30.61 wt% and the gas yield increased from 16.36 to 26.31 wt%, with increasing the reaction temperature. This is caused by secondary thermal cracking processes, followed by a series of decarboxylation, decarbonylation, deoxygenation, dehydrogenation, and alkylation. During these processes, the pyrolyzed volatiles are cleaved into smaller molecular weight organic matters [4], and to release CO₂, CO, H₂ and hydrocarbon gas [5,9].

The similar results were found in the research of other lignocellulose biomass. A study by Kim et al. [17] on fast pyrolysis of *Milkweed* in FBR showed a decrease in the bio-oil when the temperature increased from 425 °C (44.19 wt%) to 550 °C (40.74 wt%). Heidari et al. [20] reported that the optimum temperature for obtaining the highest bio-oil yield (50.8 wt%) from pyrolysis of *Eucalyptus grandis* was 450 °C. The difference in product distributions might be attributed to the differences in process conditions and the variations of biomass components.

3-2. Effect of Fluidization Velocity

The nitrogen velocity is an alternative element affecting the product yield. As known, it is used to transport pyrolysis vapor to the product-collecting zone, evading the secondary reactions [4,9]. As reported in the literature, the residence time of vapor phase in the reactor is related to the flow rates of carrier gas [9,10]. Controlling the residence time allows restricting the secondary reactions. The pyrolysis of FPR was conducted at 450 °C at the gas velocity of 1.5, 2.0, 2.5, 3.0, and 4.0 × U_{mf} correspond to the reten-

Table 2. The effect of pyrolysis temperature on product yield of FPR in BFR, feeding rate=100 g/hr, nitrogen flow rate=2.0 × U_{mf} , biomass particle size=1.0 mm

Temperature (°C)		400 °C	450 °C	500 °C	550 °C
Product yield (wt%)	Char	37.62	32.49	31.54	30.61
	Gas	16.36	16.83	22.48	26.31
	Total liquid	46.02	50.68	45.98	43.08
	Moisture (%)	33.92	39.45	41.30	47.02
	Organic (%)	66.07	60.55	58.70	52.97
Elemental analysis of bio-oil	C	49.11	53.84	54.72	55.92
	H	6.79	7.40	7.01	6.94
	N	2.14	3.33	2.28	2.79
	O	41.96	35.44	35.99	34.35
HHV of bio-oil (MJ/kg)		18.82	22.45	22.10	22.70
pH		2.80	3.02	3.05	3.37
Gas composition (mol%)	CO	31.89	30.93	26.42	25.65
	CO ₂	59.31	54.48	49.60	46.71
	H ₂	1.48	1.80	3.69	5.18
	CH ₄	5.78	10.03	16.16	18.51
	C ₂ H ₄	0.57	0.85	1.22	1.57
	C ₂ H ₆	0.43	0.93	1.55	1.30
	C ₃ H ₈	0.41	0.77	1.04	0.91
	>C ₄ hydrocarbons	0.13	0.20	0.31	0.17
HHV of gas ^a (MJ/kg)		7.78	10.38	13.59	14.34

^aThe higher heating value (HHV) of gas product [4]

Table 3. The effect of pyrolysis fluidization velocity on product yield of FPR in BFR, feeding rate=100 g/hr, reaction temperature=450 °C, biomass particle size=1.0 mm

Fluidization velocity ($U_{mf}=5.0$ L/min)		$1.5 \times U_{mf}$	$2.0 \times U_{mf}$	$2.5 \times U_{mf}$	$3.0 \times U_{mf}$	$4.0 \times U_{mf}$
Product yield (wt%)	Char	30.28	32.49	32.19	31.50	32.30
	Gas	19.74	16.83	20.28	22.55	23.36
	Total liquid	49.98	50.68	47.43	45.95	44.35
	Moisture (%)	38.99	39.45	40.27	40.81	39.72
	Organic (%)	61.01	60.55	59.73	59.19	60.28
Elemental analysis of bio-oil (wt%)	C	53.73	53.84	52.52	52.66	52.09
	H	7.12	7.40	7.08	6.90	6.95
	N	2.99	3.33	2.97	3.03	3.21
	O	36.17	35.44	37.43	37.42	37.74
HHV of bio-oil (MJ/kg)		21.88	22.45	21.19	20.98	20.81
pH		2.87	3.02	3.01	2.96	3.06
Gas composition (mol%)	CO	30.40	30.93	31.36	32.85	32.26
	CO ₂	55.12	54.48	55.22	52.93	54.06
	H ₂	1.95	1.80	1.75	1.61	1.99
	CH ₄	9.68	10.03	9.16	10.1	9.06
	C ₂ H ₄	0.88	0.85	0.77	0.76	0.79
	C ₂ H ₆	0.99	0.93	0.88	0.91	0.87
	C ₃ H ₈	0.78	0.77	0.67	0.64	0.75
	>C ₄ hydrocarbons	0.21	0.20	0.17	0.21	0.22
HHV of gas ^a (MJ/kg)		10.28	10.38	9.85	10.44	10.11

^aThe higher heating value (HHV) of gas product [4]

tion time of 2.24 s, 1.79 s, 1.44 s, 1.19 s, and 0.89 s, respectively.

Generally, raising gas velocity increases the abrasion between the bed material and sample, thereby improving the liquid yields and reducing the char yield. Moreover, the higher flow rate of gas gives the vapor phase a short time to retain in a reactor, restricting the cracking reaction and lowering the gas yield [4,9]. However, as observed in Table 3, the gas yields increased from 16.83 wt% ($2.0 \times U_{mf}$) to 23.36 wt% ($4.0 \times U_{mf}$), while the liquid yield slowly decreased from 50.68 wt% ($2.0 \times U_{mf}$) to 44.35 wt% ($4.0 \times U_{mf}$). It might be owing to the limitation of heat transmission between biomass and hot bed material [10,20]. The same trend was found by Kim et al. [17], who found an increase of liquid yield (from 42.41 to 44.94 wt%) as the gas velocity increased from 2.0 to $3.0 \times U_{mf}$. However, a diminishment in the liquid yield was found with further increase in the velocity of fluidization gas to $4.0 \times U_{mf}$. On the other hand, at faster flow rate, the pyrolysis volatiles would be blown away from the reactor without efficient condensation, causing the increase of the gas yield. The results were in agreement with the studies of lignocellulosic biomass [9,20] or algae [4,10].

3-3. Effect of Biomass Particle Size

The particle size of a sample is also a crucial factor affecting the product distribution due to its relation to heat transmission and mass transfer in the fast pyrolysis technique. The experiments were performed with three different sizes at 450 °C. As shown in Table 3, the biomass sample with a sufficiently small particle size might be heated uniformly and result in a great liquid yield. With a biomass size of (0.8-1.2) mm, the highest value of liquid product reached 50.68 wt%. An opposite result was given when the particle size was

(1.3-1.7) mm, the liquid, gas, and char yields were, respectively, 43.84 wt%, 18.95 wt%, and 37.21 wt%. These results could suggest that the larger particle size results in an inhibition for achieving the high heating rate [7,9]. The limitation of heat transfer into particle leads to an incomplete decomposition of the sample, which lowers the volatile vapor, thus producing less bio-oil yield. Furthermore, decreasing the size from (0.8-1.2) mm to (0.4-0.6) mm also reduced the yield to 45.71 wt%, whereas enhanced the gas yield to 24.01 wt%. Similarly, these trends could be found in the reports of Abbas et al. [7] and Ly et al. [9]. This is because the smaller particle exposed more area of the contact surface; therefore, it would be quickly heated as it was fed into the reactor, facilitating the degradation occurred rapidly, even sufficient time for secondary reaction to convert pyrolysis vapor into non-condensable [20]. Shen et al. [21] reported that the influence of particle size on pyrolysis is not only associated with the heat and mass transfer oppositions, but also the structure of biomass cellular and the inter-particle interplay between volatile vapor and char.

4. Compositions of Gas Product

Tables 2-4 present that CO, CO₂, and a small amount of H₂, and hydrocarbon gases (C₁-C₄) such as CH₄, C₂H₆, C₂H₄, C₃H₈, C₄H₁₀ are the major components in the gas products from the pyrolysis process of FPR with different concentration depending on the process temperature. Among these components, CO₂ was in the majority in the gas product for all experiments. The CO₂ derived from the decomposition of carboxyl groups presented in the structure of cellulose and hemicellulose in biomass. It can be observed that the selectivity of CO₂ decreased from 59.31 mol% to 46.71 mol%

Table 4. The effect of biomass particle size on product yield of FPR in BFR, feeding rate=100 g/hr, nitrogen flow rate=2.0×U_{mf}, reaction temperature=450 °C

Biomass particle size		(0.4-0.6) mm	(0.8-1.2) mm	(1.3-1.7) mm
Product yield (wt%)	Char	30.28	32.49	37.21
	Gas	24.01	16.83	18.95
	Total liquid	45.71	50.68	43.84
	Moisture (%)	38.67	39.45	43.77
	Organic (%)	61.33	60.55	56.23
Elemental analysis of bio-oil	C	53.27	53.84	57.53
	H	7.19	7.40	8.26
	N	3.17	3.33	2.03
	O	36.37	35.44	32.18
HHV of bio-oil (MJ/kg)		21.80	22.45	25.51
pH		3.11	3.02	3.28
Gas composition (mol%)	CO	34.10	30.93	24.96
	CO ₂	50.99	54.48	57.38
	H ₂	2.21	1.80	2.87
	CH ₄	10.07	10.03	10.96
	C ₂ H ₄	0.83	0.85	1.24
	C ₂ H ₆	0.98	0.93	1.44
	C ₃ H ₈	0.68	0.77	0.88
	>C ₄ hydrocarbons	0.13	0.20	0.26
HHV of gas ^a (MJ/kg)		10.69	10.38	10.93

^aThe higher heating value (HHV) of gas product [4]

Table 5. Elemental analysis and HHVs of the bio-chars from fast pyrolysis of FPR at difference temperature and particle size, with feeding rate of 100 g/hr and nitrogen flow rate of 2.0×U_{mf}

Elemental analysis of bio-char (wt%)	Reaction temperature		Biomass particle size (mm)		
	450 °C	550 °C	(0.4-0.6)	(0.8-1.2)	(1.3-1.7)
C	57.79	60.16	62.47	57.79	54.39
H	2.71	2.35	2.51	2.71	2.96
N	2.12	1.95	1.85	2.12	2.20
O ^a	5.34	2.28	4.62	5.34	6.32
Ash	32.04	34.87	28.55	32.04	34.13
HHV ^b (MJ/kg)	22.48	23.22	23.87	22.48	21.55

^aBy difference.

^bThe higher heating value (HHV) of bio-char product [13,34]

with elevated temperature from 400 to 550 °C, whereas hydrocarbon (C₁-C₄) and H₂ fractions showed the opposite trends. Higher CH₄ and H₂ species were released during the decomposition of lignin [6]. On the other hand, the increases in CH₄ and H₂ content were also attributed to the thermal cracking of aliphatic hydrocarbon and aliphatic side chain of aromatic components, and/or the demethylation of the methoxyl groups in the pyrolyzed vapors through secondary reactions, as well as breaking and rearrangement of aromatic compounds [4,10]. The results are comparable with the researches on the fast pyrolysis of woody [9] and algal materials [11]. The HHVs of produced gas were calculated based on the mole fraction and the HHV of each component in gas products [4], showing a value between 4.60 and 12.90 MJ/m³.

5. Characterization of Bio-char

Bio-chars generated from the pyrolysis of FPR were characterized. The char yield lessened with the increase of reaction temperature owing to thermal decomposition of organic components. The increase in reaction temperature facilitated the release of more volatile, enriching bio-char with more carbon. The bio-char revealed higher carbon and lower oxygen as compared to initial FPR material. Concerning the elemental analysis in Table 5, the H and O content decreased by increasing temperature while the carbon content was enhanced at the same condition. This could be explained by the enhancement of carbonization degree at high temperature. Similar behavior was also reported by other researchers [6,7].

In addition, the difference in particle size of biomass feedstock

was also concerned with the characteristics of bio-char. Table 5 shows that the percentage of carbon is inversely proportional to biomass size. A finer particle (0.4-0.6) mm contains 62.47 wt% Carbon, as considered to that of 54.39 wt% obtained from the bigger molecule (1.3-1.7) mm. The intensification of carbon concentration in bio-char as using the smaller particle size might relate to the heat exchange during pyrolysis [7]. This trend was seen in the study on pyrolysis of rice husk by Abbas et al. [7]. The ash content of bio-char was found to be higher than that in the original FPR due to the high inorganic content that remains after devolatilization of organic materials in a biomass sample [10]. The HHV of bio-char was determined according to Mott and Spooner equation (for low O content) [10,22]. The HHV was between 21.55 and 23.87 MJ/kg. These values could be compared to those of bio-char derived from the pyrolysis of other biomass such as rice husk (23.78-28.98 MJ/kg) [7], *S. japonica* macroalgae (12.59-15.53 MJ/kg) [5,10], bio-char from other woody residue such as Canadian waste saw dust (28.6 MJ/kg) [6], hornbeam residue (32.88 MJ/kg) [3], and some solid fuels such as coals (15-27 MJ/kg) [14], wood (12-18 MJ/kg), lignite (15-18 MJ/kg) [3]. With high HHV values and high carbon content, the bio-char can be used as a solid fuel. Moreover, the bio-char is more porous than biomass; thus it can be utilized to produce activated carbon and applied as catalyst support. Bio-char contains high ash; however, it was in form of mineral compounds, considered as inorganic fertilizer for cultivating farmland [10].

6. Characterization of Bio-oil

Tables 2-4 show the amount of total liquid consisted of aqueous

phase and organic phase, which were obtained from a series of condenser. The liquid product contained high amount of moisture, from 33.92 to 47.02 wt%, with increasing reaction temperature. The moisture content was formed during pyrolysis through dehydration reaction. The formation of moisture content may be explained by the intramolecular dehydration of hydroxyls in monosaccharides of biomass sample (at low temperature) and intermolecular dehydration in polymerization (at high temperature). Moreover, the generation of moisture content is also derived from the condensation at higher temperature (over 500 °C) during char formation [23].

As shown, the ultimate analysis and the HHVs of the bio-oils from FPR presented that the highly pyrolysis temperature enhance the carbon (49.11-57.53 wt%) and decrease the oxygen content (29.16-41.05 wt%) compared to those in biomass feedstock. The HHVs of bio-oils were calculated following Channiwala and Parikh's equation [9,22]. The HHV values were determined to be in the range of 18.82-25.51 MJ/kg, which was similar to those for other lignocellulose biomass: tulip tree (21.64-24.37 MJ/kg) [9], Canadian waste sawdust (25.86 MJ/kg) [6], even plastic-red oak mixture (22.95 MJ/kg) [24], and higher than those of softwood (20 MJ/kg) [25], Poplar (17.4 MJ/kg), Birch tree (16.5 MJ/kg) [26], as well as marine biomass, namely *Undaria pinnatifida* (19.30 MJ/kg) and *Prophy terena* (22.6 MJ/kg) [11]. The pH values of bio-oils from FPR were in the range of 2.80-3.37, compared to those of lignocellulosic bio-oils which were reported to be around 2 to 4. The low pH value of bio-oil was attributed to the organic acids, which were produced

Table 6. Compounds identified by GC-MS in FPR bio-oil produced by pyrolysis at 450 °C and 550 °C, nitrogen flow rate=2.0×U_{mp}, feeding rate=100 g/hr, and biomass particle size=1.0 mm

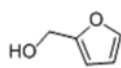
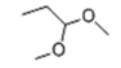
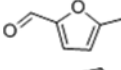
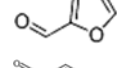
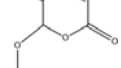
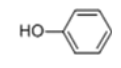
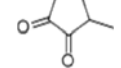
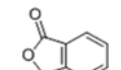
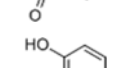
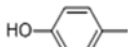
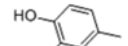
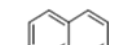
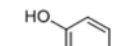
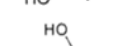
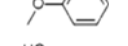
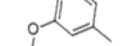
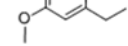
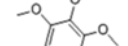
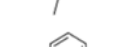
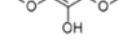
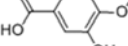
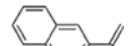
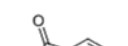
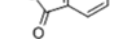
Composition of bio-oil from pyrolysis of FPR	450 °C	550 °C	Structure
	Area %		
2-Furanmethanol	1.13		
1,1-Dimethoxy propane	3.02	-	
5-Methyl-2-furfural	1.41		
Furfural	1.03		
4-Oxo-5-methoxy-2-penten-5-olide	1.56	2.67	
Phenol	1.31	1.78	
2-Hydroxy-3-methyl-2-cyclopentenone	1.80	-	
Phthalic anhydride	-	3.66	
2-Methyl phenol	0.77	1.13	

Table 6. Continued

Composition of bio-oil from pyrolysis of FPR	450 °C	550 °C	Structure
	Area %		
4-Methyl phenol	1.58	2.37	
2,4-Dimethyl phenol	1.57	2.01	
Naphthalene	0.67	1.59	
1,2-Benzenediol	2.31	1.60	
2-Methoxy-phenol	3.29	4.82	
2-Methoxy-4-methyl-phenol	2.67	4.58	
2-Methoxy-4-vinyl phenol	1.42	2.91	
4-Ethyl-2-methoxy-phenol	2.17	1.73	
3,4,5-Trimethoxy toluene	2.92	-	
2,6-Dimethoxy-Phenol	3.12	1.57	
Vanillic acid	1.39		
2-(2-Naphthyl)-1-propene		1.63	
Phthalic anhydride		3.66	
Dibutyl phthalate	1.50	0.60	
2-Methoxy-4-(1-propenyl)-Phenol	1.74	2.60	
Levogluconan	8.38	26.51	
Diethyl phthalate (DEHP)	21.33	14.70	

from the breaking of monosaccharide ring in cellulose and hemicellulose [4,27].

Bio-oils are known as complex mixtures including hundreds of

compounds with varied molecular weights. Table 6 shows the compositions of bio-oils obtained from FPR at 450 and 550 °C, analyzed by GC-MS. According to the results, the main compositions of the

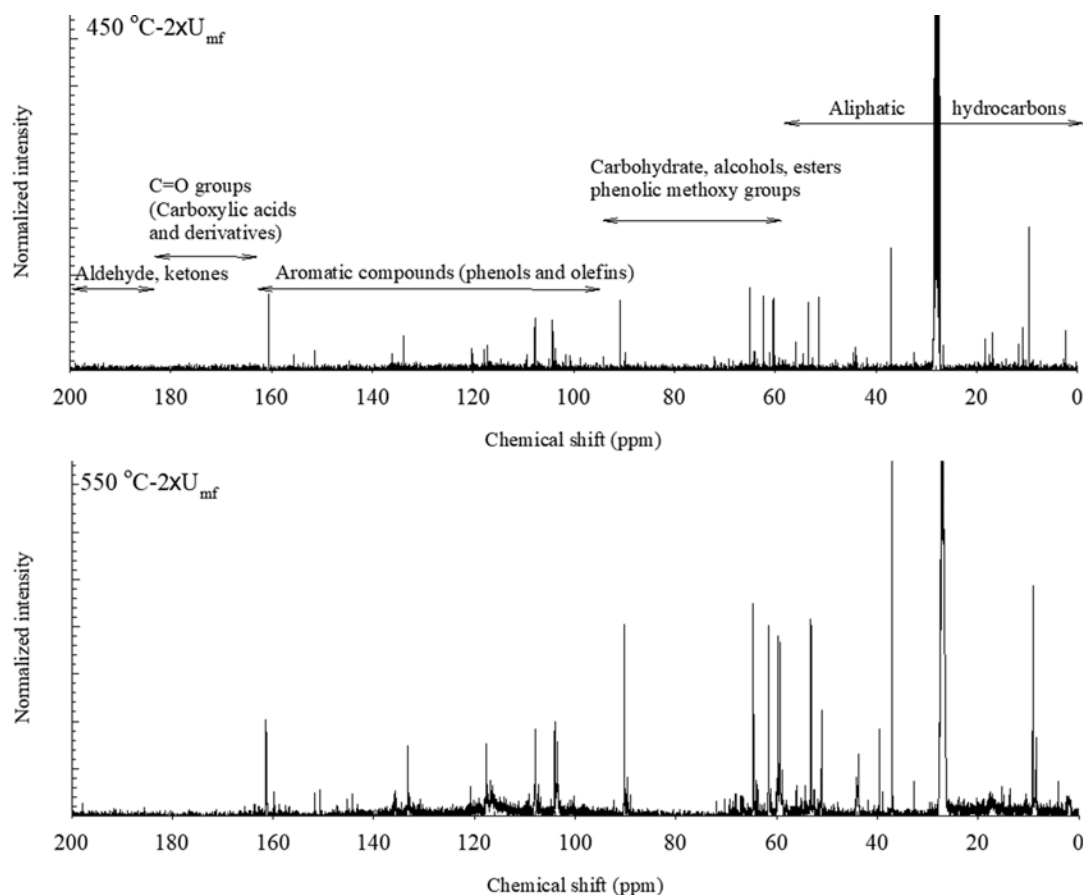


Fig. 2. ^{13}C NMR spectra of bio-oils from FPR at 450 and 550 °C.

bio-oil included dioctyl phthalate, levoglucosan, and phenolic derivatives. The most noticeable composition was dioctyl phthalate, followed by levoglucosan. The content of phthalates in the bio-oil was remarkable, which can be an advantage and different from the bio-oil of FPR compared to those from other woody biomass feedstocks. Dioctyl phthalate, known as DEHP, is a long molecule of phthalic acid ester. DEHP can be utilized as a softening agent and widely applied as plasticizers in the polymer industry to enhance the flexibility and durability of hard polyvinyl chloride plastics (PVC) [28,29]. The selectivity of dibutyl phthalate (DBP) and dioctyl phthalate (DEHP) decreased with the increase of phthalic anhydride by elevating the reaction temperature from 450 to 550 °C. This can be related to the secondary decomposition of phthalates at high temperature. In comparison with bio-oil from other woody biomass feedstocks, such as tulip tree [9], waste furniture sawdust [30] and pine sawdust [31], the FPR bio-oil showed high selectivity of phthalate composition. Levoglucosan has been considered to be a promising raw material source for the production of ethanol, for the synthesis of high value specialty chemicals in pharmaceuticals and for the biodegradable plastics production [16,32]. Bio-oils also contained considerable amounts of phenolic compounds, namely phenol, methyl-, methoxy-phenols and their derivatives, which derived from the lignin decomposition through the degradation of lignin-rich component in the FPR biomass such as bark [33]. These phenolic derivatives have good potential in different industries as a

source of chemicals, fuel or medicine production [6]. It can be seen that the levoglucosan composition increased with increased pyrolysis temperature. As known, the levoglucosan is produced through the thermal degeneration of cellulose in biomass. Additionally, the levoglucosan content obtained after reaction is proportional to the cellulose content in biomass material; it means a higher cellulose component gives a larger selectivity of levoglucosan in bio-oils [34, 35]. Therefore, the increasing temperature resulted in a promotion of decomposition reaction of cellulose, producing more levoglucosan.

The chemical functional groups in bio-oils of FPR were identified by the ^{13}C NMR method [4]. As observed in Fig. 2, the ^{13}C NMR spectra presented signals in the regions of 0-55 ppm, 55-95 ppm, and around 95-165 ppm, corresponding to function groups of aliphatic carbons, carbohydrate sugars, alcohols, esters, phenolic methoxy groups, and aromatic compounds. It can be realized that the peak intensity depends on the reaction temperature. Obviously, the higher and intense peaks observed when the temperature rose from 450 to 550 °C could be explained by the slitting of chemical bonds between carbon atoms in aliphatic hydrocarbons and higher-molecular weight compounds into shorter and lower-molecular weight compounds. Moreover, the signal in the region of aromatic compositions was found to be higher at 550 °C. During pyrolysis at high temperature, the large organic matter is broken to small and unstable fragments. These fragments, through repolym-

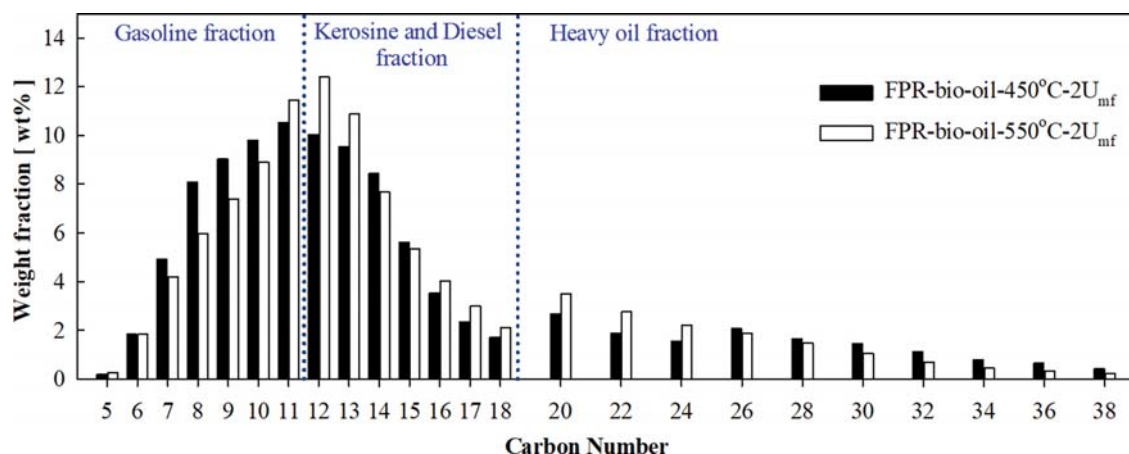


Fig. 3. Carbon number distribution of bio-oils from FPR at different temperatures, feeding rate of 100 g/hr and nitrogen flow rate of $2.0 \times U_{mf}$.

erization and aromatization reactions, tend to recombine to form the bigger and more stable ones, which are considered as aromatic compounds [16].

The carbon number distribution of bio-oils was determined using TGA with the concept of simulated distillation [9,16]. Fig. 3 shows that the carbon number of bio-oil from C_5 to C_{11} corresponds to gasoline, kerosene-diesel is the range of C_{12} - C_{18} , followed by the heavy oil fractions, in the C_{20} - C_{38} range, respectively. The distribution of these fractions in the pyrolysis bio-oil (at 450 °C) was 32.74 wt% (gasoline), 47.60 wt% (kerosene-diesel) and 19.38 wt% (heavy oil), respectively. However, with increasing temperature to 550 °C, the distribution shifted to higher carbon number, namely, the gasoline, kerosene-diesel and heavy oil fractions were found to be 39.91 wt%, 45.43 wt%, and 14.66 wt%, respectively. These results are reasonable, considering the GC-MS data and ^{13}C -NMR. The result confirms that the bio-oils from FPR could be applied as a potential source for production of alternative fuel or extracting aromatics and phenols.

CONCLUSIONS

The fast pyrolysis process of FPR was systematically investigated in a BFR. The highest value of bio-oil yield was 49.03 wt%, achieved at 450 °C with a fluidization velocity of $2 \times U_{mf}$ and sample size (0.8-1.2 mm). The HHVs of bio-oils were between 18.82 and 25.51 MJ/kg. The bio-oils contained dioctyl phthalate, levoglucosan and phenolic derivatives as major content. The ^{13}C -NMR data showed a high fraction of aromatic and aliphatic hydrocarbon. These confirm the feasibility of upgrading the bio-oil to hydrocarbon fuel. The carbon number distributions presented the weight fraction of bio-oil. The bio-char had high HHV values and high carbon content and can be utilized to produce activated carbon. This study proves the great potential of FPR for producing valuable product such as biofuel, bio-fertilizers, bio-char, and/or bio-chemicals.

ACKNOWLEDGEMENT

This research was supported by the Korea Institute of Energy Technology Evaluation and Planning (KETEP) and the Ministry of

Trade, Industry & Energy (MOTIE) of the Republic of Korea (No. 20173010092430).

NOMENCLATURE

ASTM: american society for testing and materials standard method
 X : conversion of sample material
 U_{mf} : minimum fluidization flow rate of nitrogen [L/min]

REFERENCES

- H. W. Lee, H. Jeong, Y.-M. Ju and S. M. Lee, *Korean J. Chem. Eng.*, **37**, 1174 (2020).
- S. U. Lee, K. Jung, G. W. Park, C. Seo, Y. K. Hong, W. H. Hong and H. N. Chang, *Korean J. Chem. Eng.*, **29**, 831 (2012).
- U. Morali, N. Yavuzel and S. Şensöz, *Bioresour. Technol.*, **221**, 682 (2016).
- H. V. Ly, S.-S. Kim, H. C. Woo, J. H. Choi, D. J. Suh and J. Kim, *Energy*, **93**, 1436 (2015).
- Y.-M. Kim, H. W. Lee, S. H. Jang, J. Jeong, S. Ryu, S.-C. Jung and Y.-K. Park, *Korean J. Chem. Eng.*, **37**, 493 (2020).
- R. Azargohar, K. L. Jacobson, E. E. Powell and A. K. Dalai, *J. Anal. Appl. Pyrolysis*, **104**, 330 (2013).
- Q. Abbas, G. Liu, B. Yousaf, M. U. Ali, H. Ullah, M. A. M. Munir and R. Liu, *J. Anal. Appl. Pyrolysis*, **134**, 281 (2018).
- S.-S. Kim, A. Shenoy and F. Agblevor, *Bioresour. Technol.*, **156**, 297 (2014).
- H. V. Ly, D.-H. Lim, J. W. Sim, S.-S. Kim and J. Kim, *Energy*, **162**, 564 (2018).
- H. V. Ly, S.-S. Kim, J. H. Choi, H. C. Woo and J. Kim, *Energy Convers. Manag.*, **122**, 526 (2016).
- Y. J. Bae, C. Ryu, J.-K. Jeon, J. Park, D. J. Suh, Y.-W. Suh, D. Chang and Y.-K. Park, *Bioresour. Technol.*, **102**, 3512 (2011).
- J. L. Carrasco, S. Gunukula, A. A. Boateng, C. A. Mullen, W. J. DeSisto and M. C. Wheeler, *Fuel*, **193**, 477 (2017).
- S. Papari, K. Hawboldt and R. Helleur, *Ind. Eng. Chem. Res.*, **56**, 1920 (2017).
- J. Solar, I. de Marco, B. M. Caballero, A. Lopez-Urionabarrenechea, N. Rodriguez, I. Agirre and A. Adrados, *Biomass Bioenergy*, **95**, 416

- (2016).
15. R. García, C. Pizarro, A. G. Lavín and J. L. Bueno, *Bioresour. Technol.*, **103**, 249 (2012).
16. H. V. Ly, J. H. Choi, H. C. Woo, S.-S. Kim and J. Kim, *Renew. Energy*, **133**, 11 (2019).
17. S.-S. Kim and F. A. Agblevor, *Bioresour. Technol.*, **16**, 367 (2014).
18. T. Yuzawa, C. Watanabe, R. Freeman and S. Tsuge, *Anal. Sci.*, **25**, 1057 (2009).
19. H. Yang, R. Yan, H. Chen, C. Zheng, D. H. Lee and D. T. Liang, *Energy Fuels*, **20**, 388 (2006).
20. A. Heidari, R. Stahl, H. Younesi, A. Rashidi, N. Troeger and A. A. Ghoreyshi, *J. Ind. Eng. Chem.*, **20**, 2594 (2014).
21. J. Shen, X. S. Wang, M. Garcia-Perez, D. Mourant, M. J. Rhodes and C.-Z. Li, *Fuel*, **88**, 1810 (2009).
22. S. A. Channiwala and P. P. Parikh, *Fuel*, **81**, 1051 (2002).
23. S. Wang and Z. Luo, *Pyrolysis of biomass (green alternative energy resource)*, de Gruyter Publication, China (2016).
24. Y. Xue, S. Zhou, R. C. Brown, A. Kelkar and X. Bai, *Fuel*, **156**, 40 (2015).
25. S. Papari and K. Hawboldt, *Renew. Sustain. Energy Rev.*, **52**, 1580 (2015).
26. V. Dhyani and T. Bhaskar, *Renew. Energy*, **129**, part B, 695 (2018)
27. R. Li, Z. P. Zhong, B. S. Jin and A. J. Zheng, *Bioresour. Technol.*, **119**, 324 (2012).
28. A. Gómez-Hens and M. Aguilar-Caballo, *Trends Analyt. Chem.*, **22**, 847 (2003).
29. N. Szczepańska, M. Rutkowska, K. Owczarek, J. Płotka-Wasyłka and J. Namieśnik, *Trends Analyt. Chem.*, **105**, 173 (2018).
30. G. Chang, Y. Huang, J. Xie, H. Yang, H. Liu, X. Yin and C. Wu, *Energy Convers. Manag.*, **124**, 587 (2016).
31. H. S. Heo, H. J. Park, Y. K. Park, C. Ryu, D. J. Suk, Y. W. Suk, J. H. Yim and S.-S. Kim, *Bioresour. Technol.*, **101**, S91 (2010).
32. V. A. Bridgwater, *Advances in thermochemical biomass conversion*, Springer Publication, Netherlands (1993).
33. Y. Cui, X. Hou and J. Chang, *Materials*, **10**, 668 (2017).
34. X. Zhang, W. Yang and W. Blasiak, *J. Anal. Appl. Pyrolysis*, **96**, 110 (2012).
35. Y. Wang, H. Song, L. Peng, Q. Zhang and S. Yao, *Biotechnol. Bio-technol. Equip.*, **28**, 981 (2016).